



PERFORMANCE EVALUATION OF THREE TYPES OF PASSIVE MICROMIXER WITH CONVERGENT-DIVERGENT SINUSOIDAL WALLS

Arshad Afzal

Department of Mechanical Engineering, Inha University, Nam-Gu, Incheon, Republic of Korea

Kwang-Yong Kim

Department of Mechanical Engineering, Inha University, Nam-Gu, Incheon, Republic of Korea., kykim@inha.ac.kr

Follow this and additional works at: <https://jmstt.ntou.edu.tw/journal>



Part of the [Controls and Control Theory Commons](#)

Recommended Citation

Afzal, Arshad and Kim, Kwang-Yong (2014) "PERFORMANCE EVALUATION OF THREE TYPES OF PASSIVE MICROMIXER WITH CONVERGENT-DIVERGENT SINUSOIDAL WALLS," *Journal of Marine Science and Technology*: Vol. 22: Iss. 6, Article 3.

DOI: 10.6119/JMST-014-0321-2

Available at: <https://jmstt.ntou.edu.tw/journal/vol22/iss6/3>

This Research Article is brought to you for free and open access by Journal of Marine Science and Technology. It has been accepted for inclusion in Journal of Marine Science and Technology by an authorized editor of Journal of Marine Science and Technology.

PERFORMANCE EVALUATION OF THREE TYPES OF PASSIVE MICROMIXER WITH CONVERGENT-DIVERGENT SINUSOIDAL WALLS

Acknowledgements

This work was supported by the National Research Foundation of Korea (NRF) grant (No. 20090083510) funded by the Korean government (MSIP) through Multi-phenomena CFD Engineering Research Center. Also, this work was supported by INHA UNIVERSITY Research Grant.

PERFORMANCE EVALUATION OF THREE TYPES OF PASSIVE MICROMIXER WITH CONVERGENT-DIVERGENT SINUSOIDAL WALLS

Arshad Afzal and Kwang-Yong Kim

Key words: passive micromixer, convergent-divergent sinusoidal walls, split-and-recombination, Flow separation.

ABSTRACT

A passive split-and-recombination micromixer with convergent-divergent channel walls of sinusoidal variation has been investigated using numerical simulations. With water and ethanol as working fluids, the analysis was performed using Navier-Stokes equations with convection-diffusion model in a Reynolds number range, $10 \leq Re \leq 70$. Performances of three configurations with different split-and-recombination arrangements were evaluated in terms of mixing index and pressure drop. A parametric study was also conducted with two geometrical parameters, i.e., the ratios of throat-width to diameter of circular wall and diameter of circular wall to amplitude. The results showed a significant dependence of the mixing performance on the throat-width. But, mixing performance was insensitive to the diameter of circular wall over the chosen Reynolds number range.

I. INTRODUCTION

Micromixers are widely used for various applications in the fields of lab-on-a-chip and micro-total analysis systems (μ -TAS). From the point of view of fluid dynamics, the small characteristic dimensions of the channels and the absence of turbulence make mixing a difficult task at the microscale. The Reynolds number ($Re = Ul/\nu$, where l is the characteristic cross-sectional dimension of the channel, U is the average velocity, and ν is the kinematic viscosity of the fluid) was found to be less than 100 for flows of common liquids in most of micromixers at practical pressures. Micromixers can be divided into two broad categories: active and passive. Active

systems require the application of an external force or field, i.e., pressure or temperature disturbance, magnetic energy, or electrical energy to enhance mixing. However, the active types require complex fabrication procedures and are difficult to incorporate with micro systems. In contrast, passive micromixers use the geometries of the device to produce complex flow field for effective mixing. Depending on the mode of operation, different realizations of the passive micromixers have been developed [6, 10].

Stroock *et al.* [11] used bas-relief structures on the floor of a channel to enhance the mixing process. The patterned topography was used to generate transverse flow that increases the interfacial area between the fluids to be mixed. Hu *et al.* [8] conducted numerical and experimental study of helical fluid channels with herringbone grooves etched into the bottom. The mixing behaviour of pure water and acetone solution was investigated at different Reynolds number. At $Re = 1$ and 10, nearly complete mixing was achieved in the micromixer. Jiang *et al.* [9] conducted a numerical study for flows through meandering channels with square cross-section. The study reveals a strong dependence of mixing efficiency on the secondary flow in the channel. An experimental study carried out by Howell *et al.* [7] for flow through a curved channel showed the possibility to generate lateral mixing in microfluidic systems by simply directing the flow around a bend. Chung and Shih [4] carried out numerical and experimental investigations of rhombic microchannels with splitting and recombination of fluids and flow recirculation for enhancement of mixing. Ansari *et al.* [2] studied a planar micromixer based on unbalanced split and cross-collisions of fluid streams for $10 \leq Re \leq 80$. The main channel was split into two sub-channels of unequal widths. The difference in the inertia of fluid in the sub-channels lead to the unbalanced collision of the fluid streams. The mixing was found to depend on the combined effects of unbalanced collisions and Dean vortices in the sub-channels. Also, the mixing efficiency was highest when the width of major sub-channel was twice the width of minor sub-channel.

In a recent study, Afzal and Kim [1] used convergent-divergent sinusoidal walls to improve mixing performance of

Paper submitted 09/08/13; revised 01/02/14; accepted 03/21/14. Author for correspondence: Kwang-Yong Kim (e-mail: kykim@inha.ac.kr).

Department of Mechanical Engineering, Inha University, Nam-Gu, Incheon, Republic of Korea.

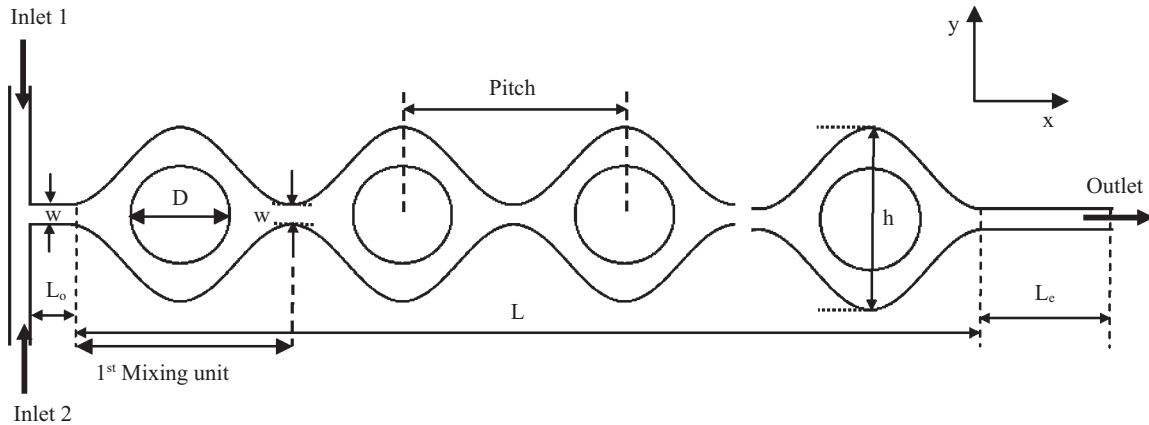


Fig. 1. Geometry of convergent-divergent micromixer [1].

a micromixer with regular split-and-recombination and Dean vortices in the sub-channels. The present study aims to investigate the mixing performance and flow characteristics of the passive micromixer [1] with three different configurations. A computational study was carried out using three-dimensional (3-D) Navier-Stokes equations for Reynolds numbers in the range, $10 \leq Re \leq 70$. Mixing index was employed to evaluate the mixing performance.

II. MICROMIXER GEOMETRY

Reference micromixer in the present study is that used by Afzal and Kim [1] shown in Fig. 1. The convergent-divergent walls are generated using a sine function of the form, $y = A \sin(2\pi x/\lambda)$ where A is the amplitude and λ is the wavelength of the sinusoidal function. The channel centerline is the axis of symmetry. The geometrical parameters related to sinusoidal walls, i.e., wavelength, λ and amplitude, A were fixed at $1120 \mu\text{m}$ and $200 \mu\text{m}$, respectively. The micromixer consists of several mixing units which are linked in series, and in each unit the channel splits into two sub-channels and recombined due to a circular cylinder located at the center of the unit. The throat-width of the convergent-divergent sections, w and diameter of the inner circular cylinder, D are geometrical parameters to be tested. The height, h of the channel depends on the amplitude of walls and is given by $(4A + 0.1) \text{ mm}$. The depth of the channel, d is $125 \mu\text{m}$ as measured in the z -direction. The cross-sectional shape of the inlet channels is a rectangle with dimensions of $0.1 \text{ mm} \times 0.125 \text{ mm}$. The axial lengths of the connecting channel (L_o), main channel (L_m), and exit channel (L_e) are 0.20 , 8.96 , and 1.50 mm , respectively. For the chosen channel length (8.96 mm), the number of mixing units is 8 . As the working fluids, ethanol and water were used in the micromixer.

The reference micromixer proposed by Afzal and Kim [1] is M1 shown in Fig. 2(a). Two different configurations of this split-and-recombination micromixer, M2 and M3, are proposed in the present work as shown in Figs. 2(b) and (c). M2 and M3, comprise of 4 and 2 split-and-recombination units, respectively, for a micromixer with 8 mixing units.

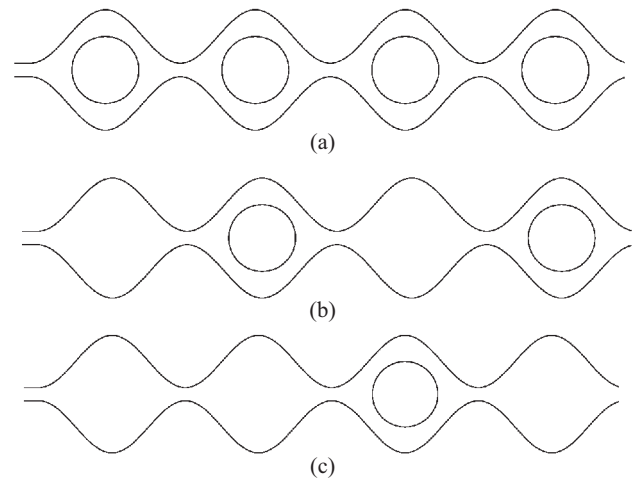


Fig. 2. Geometrical configurations of convergent-divergent micromixer: (a) M1 [1], (b) M2, and (c) M3.

III. NUMERICAL FORMULATION AND MIXING QUANTIFICATION

To investigate the flow characteristics and mixing of fluids in the micromixer, numerical simulations using 3-D Navier-Stokes equations were performed by ANSYS CFX-11 [3], a commercial computational fluid dynamics package based on the finite volume method. A multi-component model was used to calculate the concentration of the fluids in the micromixer domain. This model offers the solution for fluid mixtures with different physical properties (density, viscosity etc.). It assumes that the various components of the mixture are mixed at molecular level; however, the bulk motion of the fluid is modeled using a single velocity and pressure. The wall surface tension forces were neglected. The details of the governing equations, boundary conditions, and numerical methods can be found in Ref. 9. The properties of the working fluids (ethanol and water) used in this simulation were measured at 20°C [1, 2]. Tetrahedral cells were used to discretize the computational domain.

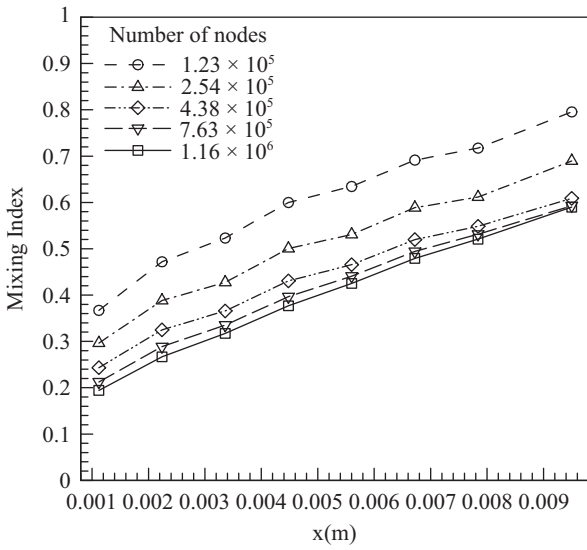


Fig. 3. Grid-dependency test for M2 (Re = 30).

A variance-based method was employed to evaluate the mixing performance of the micromixer. The variance of the mass fraction of the mixture on a cross-sectional plane normal to the flow direction can be expressed mathematically as,

$$\sigma = \sqrt{\frac{1}{N} \sum_{i=1}^N (c_i - \bar{c}_m)^2} \quad (1)$$

where N is the number of sampling points on the plane, c_i is the mass fraction at sampling points i , and \bar{c}_m is the optimal mixing mass fraction. Finally, the mixing index at any cross-sectional plane perpendicular to the axial direction is defined as,

$$M = 1 - \sqrt{\frac{\sigma^2}{\sigma_{\max}^2}} \quad (2)$$

where σ_{\max} is the maximum variance over the range of data. The mixing index varies from 0 (0% mixing) to 1 (100% mixing).

A high resolution scheme was used to discretize the advection terms in the governing equations. The SIMPLEC algorithm [12] was used for pressure-velocity coupling. The linearized algebraic system of equations resulting from the discretization was solved using a multi-grid accelerated incomplete lower upper (ILU) factorization procedure. Multi-grid techniques significantly improved the convergence behavior. The criterion for convergence was the root-mean square (RMS) residual value of 10^{-6} .

III. RESULTS AND DISCUSSION

A grid sensitivity test was performed for M2 to determine the optimum number of computational grids for spatial reso-

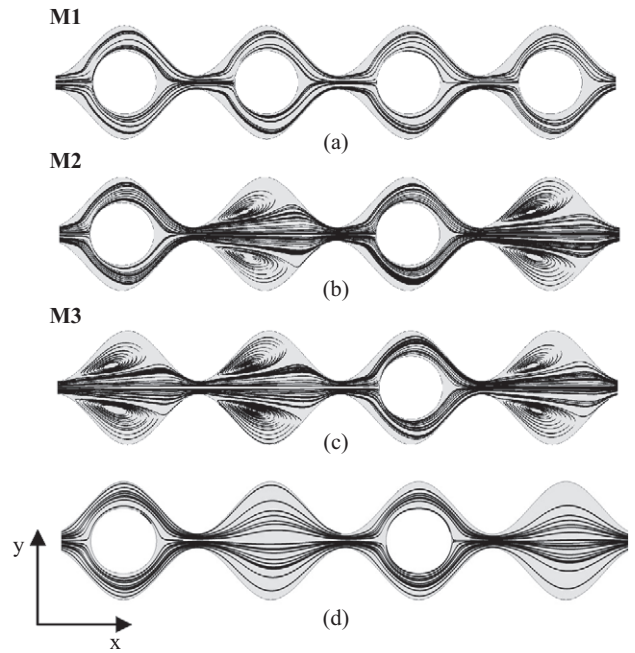


Fig. 4. Streamlines on the central xy-plane: (a) M1, (b) M2, and (c) M3 at Re = 50, and (d) M2 at Re = 10.

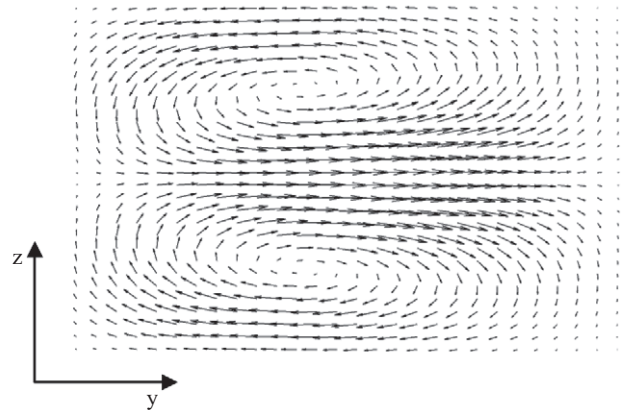


Fig. 5. Typical pattern of secondary flow.

lution. The grid system with 7.63×10^5 nodes was found to be optimum from the results of the test for variation of mixing index with the channel length as shown in Fig. 3.

The fluid mixing in the convergent-divergent microchannel with sinusoidal walls with different split-and-recombination arrangements (M1, M2, and M3 in Fig. 2) was analyzed for $A = 0.20$ mm in Fig. 4, which shows streamlines on the central xy-plane at Re = 50. In configuration M1, Dean vortices [5] appear in the sub-channels, which cause bending of streamlines at Re = 50. Centrifugal forces act on the fluid flows in the sub-channels. Due to the differential centrifugal forces, secondary flows (known as Dean's vortices) evolve on the transverse planes of each sub-channel. A typical flow pattern of the secondary flows on the transverse planes consists of two counter-rotating vortices as shown in Fig. 5. Dean

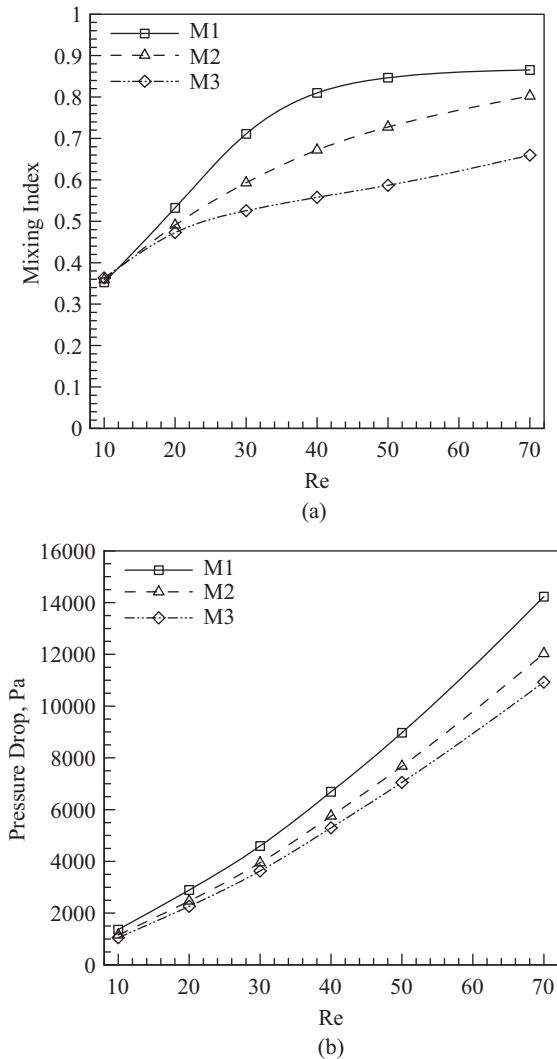


Fig. 6. Mixing index at the exit and pressure drop versus Reynolds number for configurations M1, M2 and M3: (a) mixing index at the exit and (b) pressure drop.

vortices are characterized by a finite Dean number, κ , defined as $Re(l/R)^{1/2}$, where l is the characteristic cross-sectional dimension of the channel and R is the radius of curvature. It should be noted that smaller radius of curvature and/or higher Reynolds number result in higher Dean number, therefore, a stronger secondary motion. The recirculation zones act as micro-stirrers for the ethanol and water streams and Dean vortices increase the interfacial area of the fluid streams, thereby facilitating faster diffusion and enhancing mixing. The recirculation zones are found in the recesses of M2 and M3 at $Re = 50$ (Figs. 4(b) and (c)), but they are not found in M2 at $Re = 10$ (Fig. 4(d)). Therefore, it is interesting to find the effect of the flow recirculation in the recesses on the mixing performance compared to that of the split-and-recombination.

Fig. 6 shows variations of mixing index at the exit of the micromixer with Reynolds number for M1, M2, and M3. To

determine the mixing index, the exit plane was placed at 3.0 mm downstream of the end of the last mixing segment. It can be seen that the mixing index increases as the number split-and-recombination units increases regardless of the Reynolds number, and thus M1 shows highest mixing indexes. This indicates that the flow recirculation is less effective on the mixing of fluids than the split-and-recombination. The overall pressure drop shown in Fig. 6(b) is important in micromixer designs, especially for the integration of the device with micro-analysis systems. The pressure drops were calculated by the difference in area-averaged total pressure on the cross-sectional plane between the inlet and exit of the mixing channel. In Fig. 6(b), the pressure drop also increases as the number of the split-and-recombination units increases regardless of the Reynolds number, and thus the configuration M3 shows best performances in terms of pressure drop. Therefore, a compromise between the mixing performance and pressure drop is necessary in the design of the split-and-recombination micromixer.

Fig. 7 shows ethanol mass fraction distributions on cross-sectional planes at the ends of 2nd, 4th, 6th, and 8th mixing units (Fig. 1) of the micromixer. The distribution in M2 at $Re = 10$ indicates that the centrifugal forces are weak and the fluids are mixing primarily by diffusion due to low Reynolds number. However, at $Re = 50$, the concentration layers in the sub-channels are affected by secondary flows in configuration M1, and combined secondary and recirculation flows affect the mixing performances of configurations M2 and M3. The recirculation zones act as micro-stirrers for the ethanol and water streams, and Dean vortices causes distortion of concentration contours [1]. M3 shows the fastest development of mixing along the axis of the micromixer at $Re = 50$ among the tested configurations.

The mixing behavior and pressure drop in the micromixer M2 was investigated in the Reynolds number range, $10 \leq Re \leq 70$ for three different amplitudes of the channel walls, $A = 0.15, 0.2,$ and 0.25 mm. Fig. 8(a) shows variations of the mixing index at the exit of the micromixer with Reynolds number. The previous work on configuration M1 [1] reported that the increase in the amplitude results in the increase in the intensity of secondary motion. This trend is also found in the configuration M2. The design with $A = 0.25$ mm shows the maximum mixing index over the entire Reynolds number range, $10 \leq Re \leq 70$. At $Re = 10$, mixing is primarily performed by diffusion. With increase in Reynolds number in the tested range, the mixing performance is found to increase for all amplitudes. Fig. 8(b) shows the variations of pressure drop with Reynolds number for the three different amplitudes. The pressure drop commonly increases with Reynolds number, and decreases with amplitude of the channel walls. The design with the highest amplitude ($A = 0.25$ mm) shows the lowest pressure drop throughout the Reynolds number range considered. Therefore, higher amplitude channels are preferable in terms of both mixing performance and pressure loss.

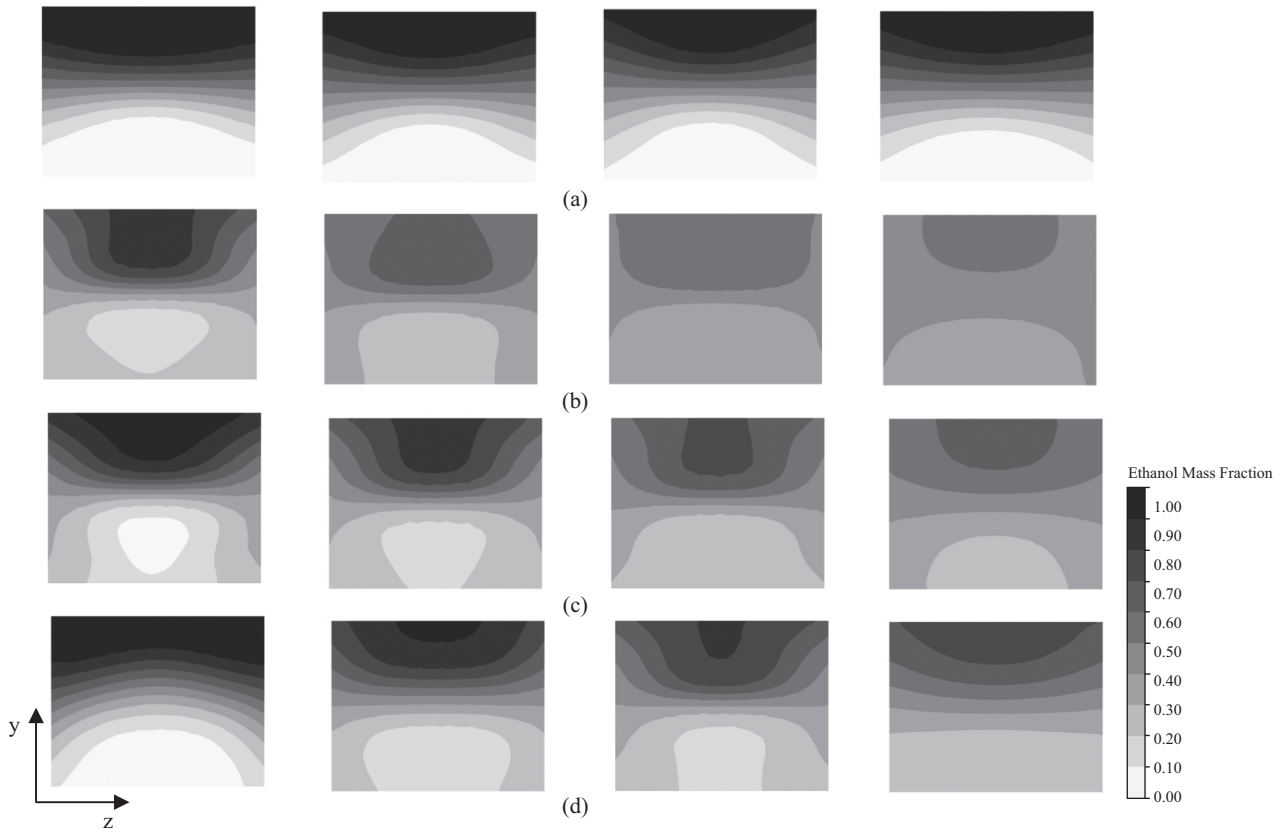


Fig. 7. Ethanol mass fraction distributions on cross-sectional planes at the ends of 2nd, 4th, 6th, and 8th mixing units (from left to right): (a) M2 at Re = 10 and (b) M1, (c) M2, and (d) M3 at Re = 50.

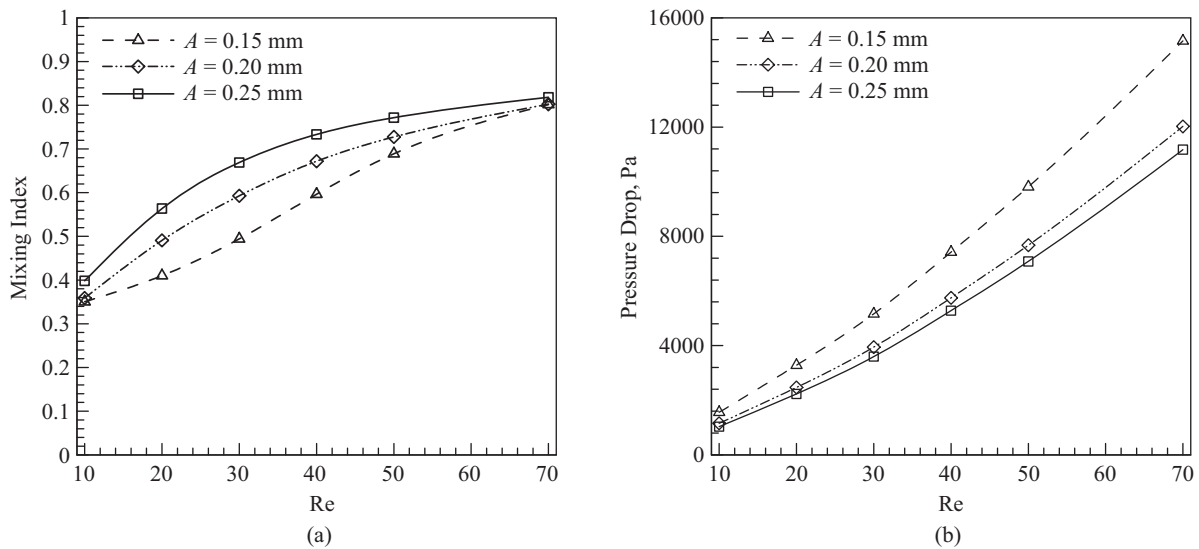


Fig. 8. Variations of mixing index at the exit and pressure drop in M2 with Reynolds number for different amplitudes: (a) mixing index at the exit and (b) pressure drop.

The mixing behavior of the micromixer M1 was investigated for three different values of the ratio of throat-width to diameter of circular wall, w/D and ratio of diameter of circular wall to amplitude, D/A for the Reynolds number range, $10 \leq$

$Re \leq 70$ in Figs. 9(a) and (b), respectively. As can be seen in Fig. 9(a), the mixing index is very sensitive to w/D . With increase in w/D , the mixing quality deteriorates in the entire Re range considered. The increase in w/D causes the increase

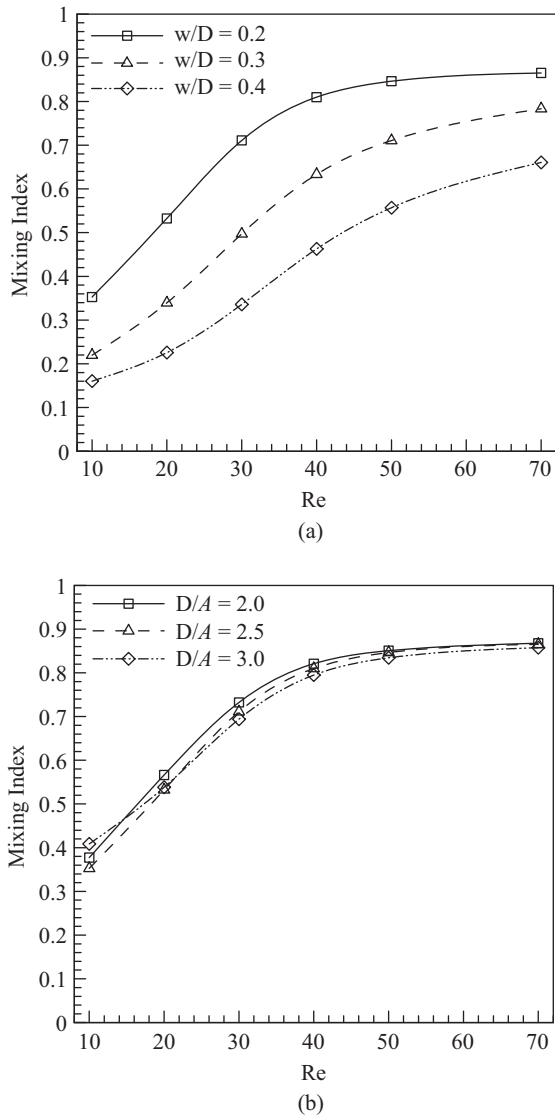


Fig. 9. Dependency of mixing index at the exit on w/D and D/A at different Reynolds numbers for configuration M1: (a) w/D and (b) D/A .

in the effective diffusion distance for low Reynolds numbers, while it causes the decrease in the intensity of secondary motion for high Reynolds numbers in the Re range considered. However, the mixing index remains almost invariant with variation of D/A . Maximum variation in the mixing index is less than 5% in the entire parametric space of D/A and Re .

For the reference micromixer [1], it has been shown that two different kinds of secondary motion affect the mixing performance in the micromixer, viz. the Dean vortices originating in the sub-channels and a symmetric double vortex pair at the throat of the convergent-divergent channel. Streamlines inside the microchannel are shown in Fig. 10. It can be seen that the bending of streamlines occurs on account of secondary motion. At a fixed w/D , the strength of secondary motion is proportional to Reynolds number [1]. For $w/D = 0.2$, the

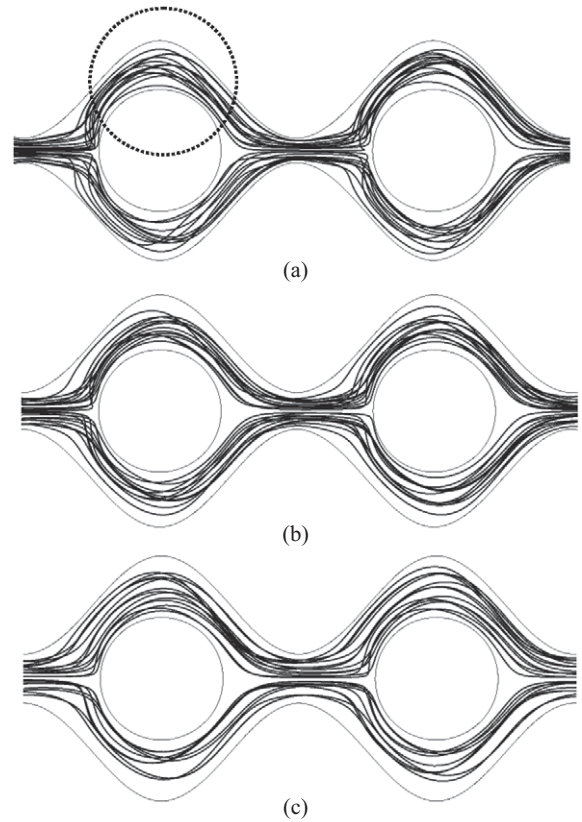


Fig. 10. Streamlines in the channel at $Re = 50$ for configuration M1: (a) $w/D = 0.2$, (b) $w/D = 0.3$ and (c) $w/D = 0.4$.

bending of streamlines is considerably higher than $w/D = 0.4$ which clearly indicates a stronger secondary motion for narrow channels (low w/D) at $Re = 50$. Fig. 11 shows the double-symmetric vortex pairs in terms of velocity vectors on a cross-sectional plane at the throat of convergent-divergent channel at $Re = 50$. The qualitative flow patterns are nearly similar for chosen w/D ratios. However, the scales for the vortical motion suggest a decrease in the intensity with increasing w/D . Thus, it can be concluded that the enhanced mixing performance at $w/D = 0.2$ is related to stronger secondary flows in the sub-channels and throat acting over a reduced diffusion distance, compared to $w/D = 0.4$.

IV. CONCLUSIONS

A passive micromixer using split-and-recombination with convergent-divergent walls of sinusoidal variation was investigated in a Reynolds number range, $10 \leq Re \leq 70$ using Navier-Stokes analysis. Mixing performance and pressure drop were evaluated for three different configurations of the micromixer, and effects of geometrical parameters, i.e., the ratio of throat-width to diameter of circular wall, w/D and ratio of diameter of circular wall to amplitude, D/A on mixing performance were analyzed. It was found that both the mixing index at the exit of the micromixer and pressure drop in-

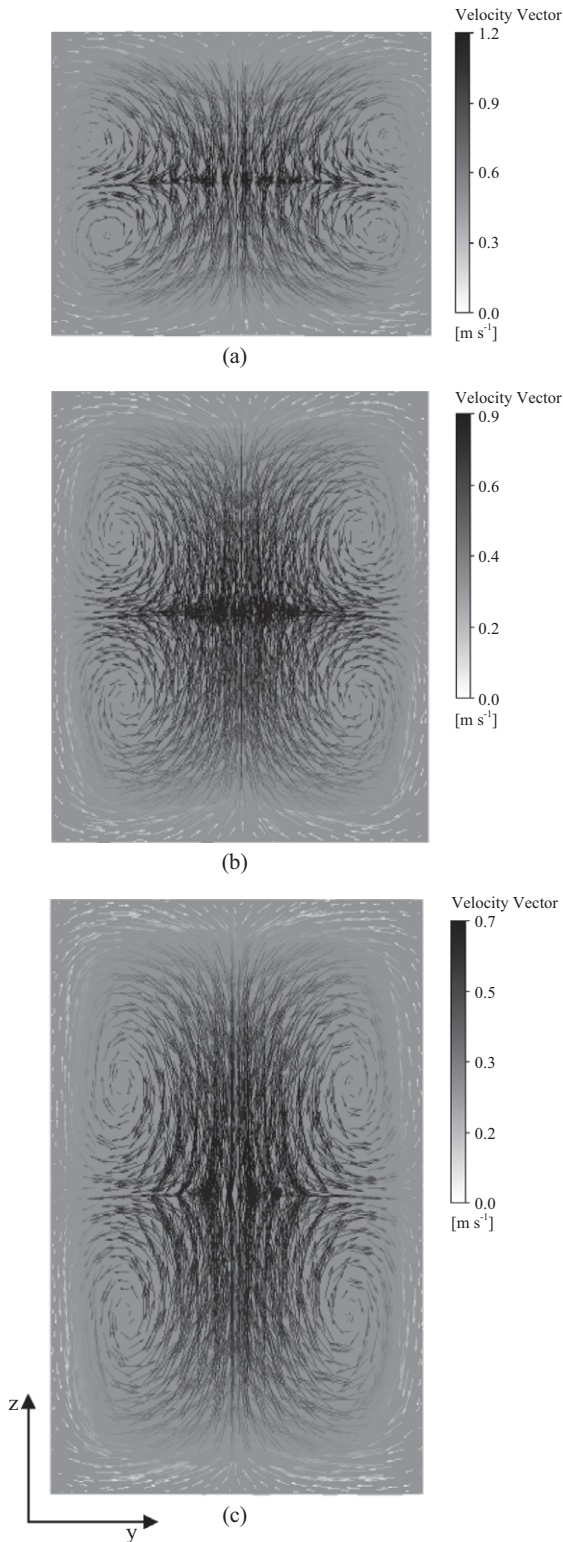


Fig. 11. Velocity vectors on y - z plane at $Re = 50$ for configuration M1: (a) $w/D = 0.2$, (b) $w/D = 0.3$ and (c) $w/D = 0.4$.

crease as the number split-and-recombination units increases regardless of the Reynolds number. Therefore, a compromise between the mixing performance and pressure drop is necessary in the design of the split-and-recombination micromixer. The higher amplitude channels showed the better performances in both mixing and pressure loss. The mixing index at the exit was strongly dependent on w/D , and deteriorated with increase in w/D in the entire Re range considered. However, maximum variation in the mixing index was less than only 5% in the entire parametric space of D/A and Re .

ACKNOWLEDGMENT

This work was supported by the National Research Foundation of Korea (NRF) grant (No. 20090083510) funded by the Korean government (MSIP) through Multi-phenomena CFD Engineering Research Center. Also, this work was supported by INHA UNIVERSITY Research Grant.

REFERENCES

1. Afzal, A. and Kim, K.-Y., "Passive split and recombination micromixer with convergent-divergent walls," *Chemical Engineering Journal*, Vol. 203, pp. 182-192 (2012).
2. Ansari, M. A., Kim, K.-Y., Anwar, K., and Kim, S. M., "A novel passive micromixer based on unbalanced splits and collisions of fluid streams," *Journal of Micromechanics and Microengineering*, Vol. 20, pp. 1-10 (2010).
3. CFX-11.0, *Solver Theory*, ANSYS (2007).
4. Chung, C. K. and Shih, T. R., "Effect of geometry on fluid mixing of the rhombic micromixers," *Microfluidics and Nanofluidics*, Vol. 4, pp. 419-425 (2008).
5. Dean, W. R., "Note on the motion of a curved pipe," *Philosophical Magazine*, Vol. 4, pp. 208-223 (1927).
6. Hessel, V., Lowe, H., and Schönfeld, F., "Micromixers - a review on passive and active mixing principles," *Chemical Engineering Science*, Vol. 60, pp. 2479-2501 (2005).
7. Howell, Jr., P. B., Mott, D. R., Golden, J. P., and Ligler, F. S., "Design and evaluation of a Dean vortex-based micromixer," *Lab on a Chip*, Vol. 4, pp. 663-669 (2004).
8. Hu, Y. H., Hwu, F. S., and Lin, K. H., "Two fluid mixing in a micromixer with helical channel and grooved surfaces," *Proceedings of the 2nd International Conference on Engineering and Technology Innovation*, pp. 285 (2012).
9. Jiang, F., Drese, K. S., Hardt, S., Küpper, M., and Schönfeld, F., "Helical flows and chaotic mixing in curved micro channels," *AIChE Journal*, Vol. 50, pp. 2297-2305 (2004).
10. Nguyen, N. T. and Wu, Z., "Micromixers - a review," *Journal of Micromechanics and Microengineering*, Vol. 15, R1- R16 (2005).
11. Stroock, A. D., Dertinger, S. K., Ajdari, A., Mezic, I., Stone, H. A., and Whitesides, G. M., "Chaotic mixer for microchannels," *Science*, Vol. 295, pp. 647-651 (2002).
12. Van Doormaal, J. P. and Raithby, G. D., "Enhancement of the SIMPLE method for predicting incompressible fluid flows," *Numerical Heat Transfer*, Vol. 7, pp. 147-163 (1985).